Design and Synthesis of 2-Amino-4-methylpyridine Analogues as Inhibitors for Inducible Nitric Oxide Synthase and in Vivo Evaluation of [^{18}F]6-(2-Fluoropropyl)-4-methyl-pyridin-2-amine as a Potential PET Tracer for Inducible Nitric Oxide Synthase

Dong Zhou,[†] Hsiaoju Lee,[†] Justin M. Rothfuss,[†] Delphine L. Chen,[†] Datta E. Ponde,[†,‡] Michael J. Welch,[†] and Robert H. Mach*,[†]

Division of Radiological Sciences, Washington University School of Medicine, Campus Box 8225, 510 South Kingshighway Boulevard, St. Louis, Missouri 63110

Received December 9, 2008

A series of position-6 substituted 2-amino-4-methylpyridine analogues was synthesized and compounds **9**, **18**, and **20** were identified as the inhibitors with the greatest potential to serve as PET tracers for imaging inducible nitric oxide synthase (iNOS). [^{18}F]**9** was synthesized and evaluated in a mouse model of lipopolysaccharide (LPS)-induced iNOS activation. In vivo biodistribution studies of [^{18}F]**9** indicate higher tracer uptake in the lungs of the LPS-treated mice when compared to control mice. Tracer uptake at 60 min postinjection was reduced in a blocking study using a known inhibitor of iNOS. The expression of iNOS was confirmed by Western blot analysis of lung samples from the LPS-treated mice. MicroPET studies also demonstrated accumulation of radiotracer in the lungs of the LPS-treated mice. Taken collectively, these data suggest that [^{18}F]**9** shows favorable properties as a PET tracer to image iNOS activation with PET.

Introduction

Nitric oxide (NO[a]) is an important and unique mediator of a variety of physiological and pathological processes.[1] NO is generated from the oxidation of L-arginine to L-citrulline in a two-step process by nitric oxide synthase (NOS) enzymes.[2] In the NOS family, there are two constitutive isozymes of NOS, neuronal NOS (nNOS) and endothelial NOS (eNOS), and one inducible isozyme (iNOS). The three isozymes of NOS are expressed in different tissues to generate NO for specific physiological roles. nNOS generates NO as a neurotransmitter and neuromodulator, mainly in brain and peripheral nerve cells; eNOS regulates blood pressure, primarily in vascular endothelial cells;[3] iNOS is induced by various inflammatory stimuli (e.g., endotoxin) in activated macrophages and other types of cells and plays an crucial role in the host defense and the inflammatory processes.

Normally, the basal level of NO in all parts of the body is very low, mainly due to the constitutive nNOS and eNOS. In contrast, once expressed, iNOS can continue to generate NO in large amounts (up to μM concentrations) for a prolonged period of time.[4] Studies have shown that production of NO by iNOS is implicated in a variety of acute and chronic inflammatory diseases (e.g., sepsis, septic shock, vascular dysfunction in diabetes, asthma, arthritis, multiple sclerosis, and inflammatory diseases of the gut);[5] iNOS activity has also been found in many tumors.[6] Because of the central role of iNOS in NO-related diseases, numerous efforts have been made to develop iNOS inhibitors as pharmaceuticals ranging from the nonselective L-arginine analogues[7] to the selective inhibitors reported recently.[8] Some inhibitors of iNOS have shown promising results in animal models of sepsis, lung inflammation, arthritis, and autoimmune diabetes.[8c] Therefore, the development of a radiolabeled iNOS inhibitor for probing iNOS expression in vivo using noninvasive positron emission tomography (PET) imaging will be of tremendous value to the study and treatment of NO-related diseases.

Chart 1

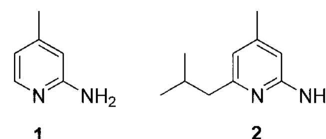

PET is being used more frequently in clinical and research studies because of its high sensitivity, good spatial resolution, and ease in accurate quantification. Additionally, the absence of a physiologic effect from the radiotracers makes it a safe in vivo imaging tool. When short-lived positron-emitting radionuclides (^{18}F $t_{1/2}$ = 109.8 min and ^{11}C $t_{1/2}$ = 20.4 min) are incorporated into biologically active molecules (e.g., iNOS inhibitors), they can be used as tracers that target those physiological pathways. 2-Amino-4-methylpyridine (**1**) has been reported as a nonselective NOS inhibitor with good potency,[9] while the 6-substituted alkyl analogues of **1** have slightly improved potency and selectivity over the parent compound; analogue **2** has the best potency (IC_{50} against iNOS = 28 nM) (Chart 1).[10] Computational calculations suggest that the position-6 is the most tolerant position to introduce a substitutent[11] that would be suitable for radiolabeling with PET radionuclides ^{18}F and ^{11}C.

In the past decade, the development of radiolabeled PET tracers for iNOS has been limited[12] compared with the relatively rapid development of novel iNOS inhibitors as pharmaceuticals. In this paper, we describe the synthesis and screening of a series of position-6 substituted 2-amino-4-methylpyridine analogues

* To whom correspondence should be addressed. Phone: (314) 362-8538. Fax: (314) 362-0039. E-mail: rhmach@mir.wustl.edu.

† Division of Radiological Sciences, Washington University School of Medicine.

‡ Current address: Department of Radiology, University of Pennsylvania, 420 Curie Boulevard, Philadelphia, Pennsylvania 19104.

[a] Abbreviations: NO, nitric oxide; NOS, nitric oxide synthase; iNOS, inducible nitric oxide synthase; eNOS, endothelial nitric oxide synthase; nNOS, neuronal nitric oxide synthase; LPS, lipopolysaccharide; PET, positron emission tomography; DAST, diethylaminosulfur trifluoride; PBSF, perfluorobutane sulfonyl fluoride; SEITU, *S*-ethylisothiourea; L-NIL, L-N^6-(1-iminoethyl)lysine; 2-AP, 2-aminopyridine.

10.1021/jm801556h CCC: $40.75 © 2009 American Chemical Society
Published on Web 03/26/2009

Scheme 1[a]

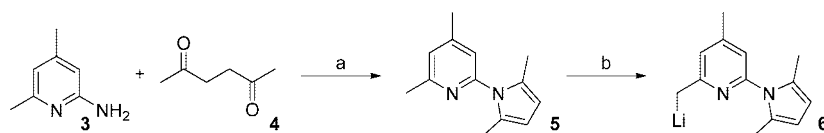

[a] Reagents and conditions: (a) HOAc, toluene, reflux; (b) *n*-BuLi, Et_2O, −20 to −10 °C.

Scheme 2[a]

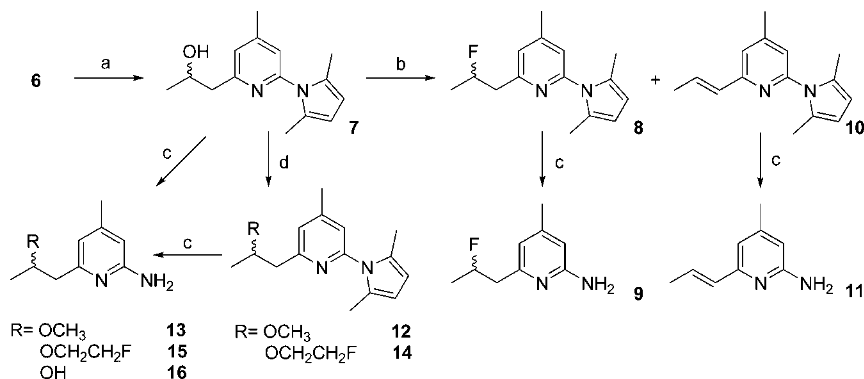

[a] Reagents and conditions: (a) CH_3CHO, Et_2O, −78 °C to RT; (b) DAST, CH_2Cl_2 or PBSF, $(NEt_3)(HF)_3$, Et_3N, CH_3CN; (c) $NH_2OH\cdot HCl$, EtOH, H_2O; (d) CH_3I or $BrCH_2CH_2F$, NaH, THF.

Scheme 3[a]

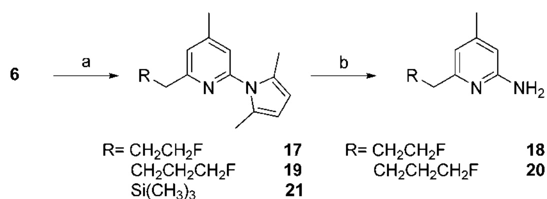

[a] Reagents and conditions: (a) **17**: $BrCH_2CH_2F$; or **19**: $BrCH_2CH_2CH_2F$; or **21**: $(CH_3)_3SiCl$, Et_2O. (b) $NH_2OH\cdot HCl$, EtOH, H_2O.

as potential PET tracers for imaging iNOS, the radiosynthesis of [^{18}F]**9**, and the in vivo evaluation of [^{18}F]**9** in a mouse model of lipopolysaccharide (LPS)-induced iNOS activation.

Results and Discussion

Chemistry. The previously reported method was applied to synthesize the key intermediate **6** (Scheme 1).[10] Compound **6** reacted with acetaldehyde to afford **7** in high yield (Scheme 2). Compound **7** was converted to **8** using diethylaminosulfur trifluoride (DAST) or perfluorobutane sulfonyl fluoride (PBSF) as the fluorinating agents. Compound **10** was obtained as a byproduct in both cases and was formed as the major product when PBSF was used as the fluorinating agent. These results indicate the facile elimination to form a conjugated double bond adjacent to the pyridine ring. The conversion of the OH in **7** to Br using PPh_3 and CBr_4 failed to give the expected product (data not shown). Compounds **12** and **14** were synthesized from **7** via O-alkylation using CH_3I and $BrCH_2CH_2F$, respectively, in the presence of CaH_2 (Scheme 2). The pyrrole protecting group in all the 2-amino pyridine analogues was removed by refluxing in an aqueous ethanol solution of hydroxylamine hydrochloride as previous reported.[11] Although no details were given in the reference, we found that a 2:1 mixture of ethanol and water (containing 4M $NH_2OH\cdot HCl$) at 110 °C afforded good results. The nucleophilic substitutions of $BrCH_2CH_2F$, $BrCH_2CH_2CH_2F$, and $(CH_3)_3SiCl$ by **6** afforded **17**, **19**, and **21**, respectively, in high yields (Scheme 3). Among the compounds synthesized, **9**, **13**, **15**, **16**, **27**, **30**, and **33** are racemic mixtures, which were used without chiral resolution in the following studies.

The Peterson olefination reaction[13] using α-trimethylsilyl carbanion **22** and the corresponding ketones was used to synthesize **23**, **25**, **28**, and **31**, respectively (Scheme 4). Compound **22** was synthesized by reacting **21** with 1 equiv of *n*-butyl lithium in good yield, which was evidenced by the good yield of **23** following the reaction with acetone. *E*/*Z* isomers were observed in these reactions, and the isomers were reduced either by ammonium formate/ethanol in the presence of palladium on carbon (**25** and **28**) or by magnesium in ethanol (**31**). The former method was unsuccessful for the synthesis of **32**, most likely due to the poisoning of the palladium catalyst by the sulfur atom in **31**.

The synthesis of precursor **38** for the nucleophilic labeling of [^{18}F]**9** is shown in Scheme 5. The hydroxyl group in the 2-hydroxypropyl group had to be protected as the corresponding acetate ester during the reaction with di-*tert*-butyldicarbonate (Boc_2O). Without protection of the −OH, **37** was only a minor product, with the major product as the corresponding *t*-butylcarbonate and other byproduct (data not shown). The acetylation to make **34** from **7** using acetyl chloride was slow and the yield was only 39%, probably due to steric hindrance from the secondary alcohol and the pyridine ring. A more efficient method of making **34** involved treating **6** with acetaldehyde followed by treatment with ethyl acetate to give **34** in an overall yield of 43%.

The synthesis of the mesylate and tosylate precursors required for the radiosynthesis of [^{18}F]**18** failed to afford the desired products. It was found that the mesylate precursor formed initially but converted quickly even at room temperature to a cyclic 1-substituted pyridinium via an internal nucleophilic attack of the mesylate group by the pyridine nitrogen atom, and this cyclized product was confirmed by mass spectrometry, ^{1}H NMR, and elemental analysis (data not shown). Therefore, attempts to radiolabel **18** were not successful and our efforts focused on radiolabeling **9** with ^{18}F.

Scheme 4[a]

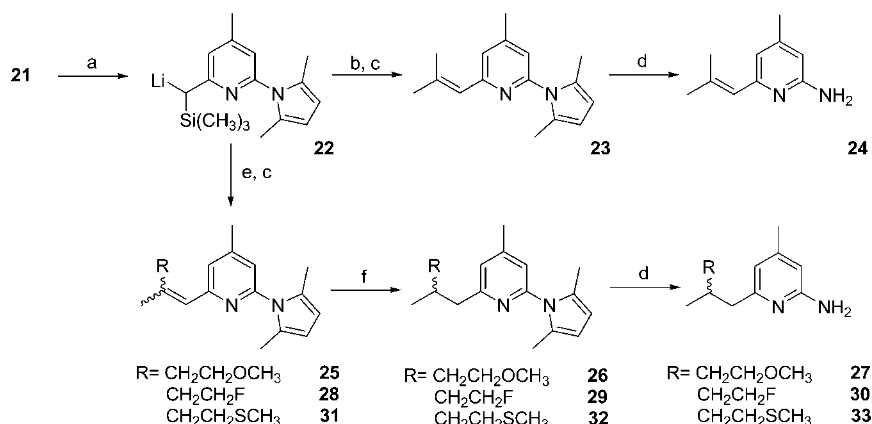

[a] Reagents and conditions: (a) *n*-BuLi, Et_2O, −20 °C. (b) Acetone, Et_2O, −78 °C to RT. (c) 1 N HCl. (d) $NH_2OH \cdot HCl$, EtOH, H_2O. (e) **25**: $CH_3COCH_2CH_2OCH_3$; **28**: $CH_3COCH_2CH_2F$; or **31**: $CH_3COCH_2CH_2SCH_3$, Et_2O, −78 °C to RT. (f) $HCOONH_4$, Pd/C, EtOH, 80 °C (**25**, **28**); or Mg, EtOH (**31**).

Scheme 5[a]

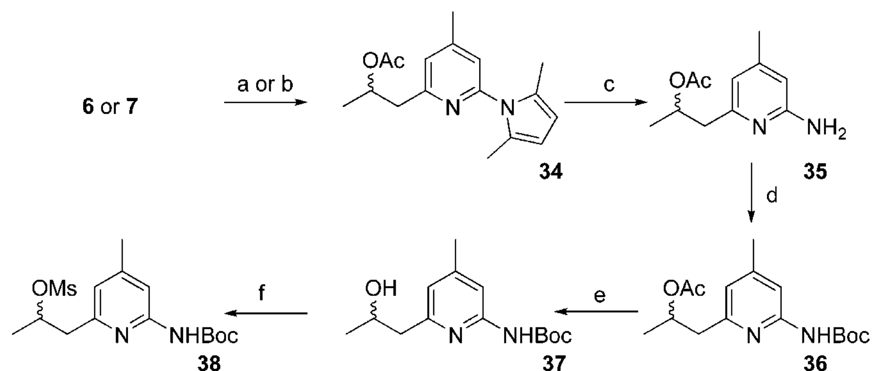

[a] Reagents and conditions: (a) **6**: CH_3CHO, Et_2O, −78 °C to RT; then AcOEt, Et_2O. (b) **7**: AcCl, Et_3N, CH_2Cl_2. (c) $NH_2OH \cdot HCl$, EtOH, H_2O. (d) Boc_2O, *t*-BuOH. (e) K_2CO_3, MeOH, H_2O. (f) MsCl, Et_3N, CH_2Cl_2.

Scheme 6[a]

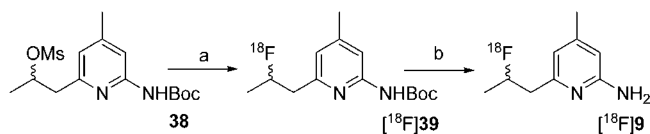

[a] Reagents and conditions: (a) [^{18}F]fluoride, K_2CO_3, K_{222}, CH_3CN, 110 °C; (b) 1 N HCl, microwave.

Radiosynthesis of [^{18}F]9. [^{18}F]**9** was synthesized via a nucleophilic substitution of the mesylate precursor **38** with [^{18}F]fluoride, followed by deprotection with 1 N HCl (Scheme 6). The incorporation of [^{18}F]fluoride was only 10−20% at optimized conditions; however, after reversed-phase HPLC purification, [^{18}F]**9** was obtained in high chemical and radiochemical purity. The specific activity was >1000 mCi/μmol at the end of synthesis. The total synthesis and purification time was 120 min, and the isolated yield was up to 10% (decay corrected). The low incorporation of [^{18}F]fluoride should be due to the slow rate of nucleophilic substitution on the secondary carbon and the base-catalyzed elimination to form the corresponding nonreactive olefin. The radiolabeling using acetonitrile as the solvent gave a higher yield than that in DMF; use of the corresponding tosylate and triflate precursors gave a much lower yield or no incorporation of ^{18}F at all.

In Vitro Enzyme Assays. The inhibition potency for recombinant iNOS, eNOS, and nNOS was determined using a commercial nitric oxide synthase screening kit (GE Healthcare Biosciences Corporation, Piscataway, NJ) following the manufacturer's protocol with minor modifications. The assay was validated using standard NOS inhibitors. Only the most potent iNOS inhibitors were further evaluated for eNOS and nNOS potency to determine the selectivity between iNOS and eNOS or nNOS.

As shown in Table 1, the most potent compound for iNOS was **18**, with approximately 30-fold selectivity against eNOS and 10-fold against nNOS; **9** and **20** showed less potency for iNOS and less selectivity against eNOS and nNOS but were comparable to the previously reported compound **2**, which had a potency of IC_{50} = 193 nM for iNOS in our assay (The reported IC_{50} of **2** is 28 nM[10]). We cannot determine the reasons for the difference between our value and the reported data, but slow time-dependent inhibition has been frequently reported.[8b,11,14,15] The IC_{50} value may be influenced by the incubation time; longer incubation time may deliver more potent IC_{50} values. Additionally, the measured inhibition potency may depend on the concentrations of NADPH and L-arginine.[15] Nevertheless, the assay was validated by standard iNOS inhibitors (Table 1), and **9**, **18**, and **20** were identified as potential PET tracers for imaging iNOS according to our assay results.

It has been reported previously that the 6-position of the pyridine ring has the greatest amount of bulk tolerance with respect to potency for inhibiting iNOS. Therefore, several 6-substituted analogues were synthesized in order to further investigate this structure−activity relationship. When the 2′-methyl group in lead compound **2** was replaced with a fluorine

Table 1. IC_{50} values of the 2-Amino-4-Methylpyridine analogues[a]

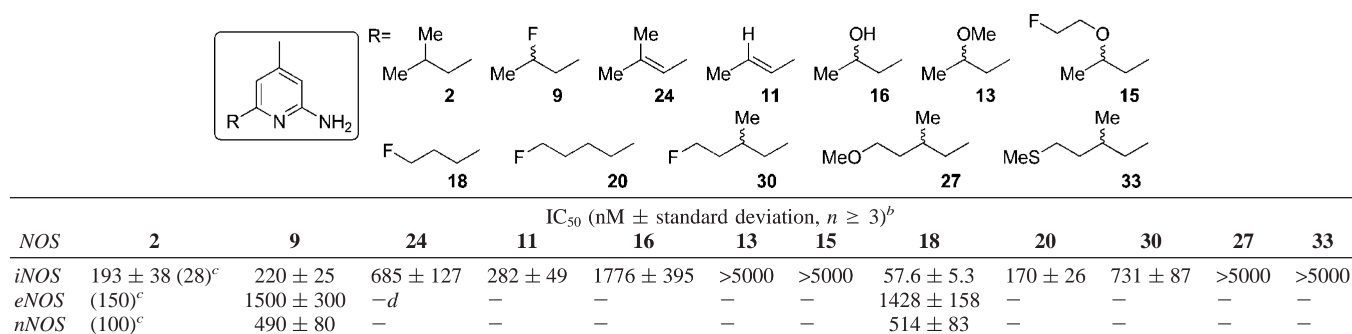

NOS	2	9	24	11	16	13	15	18	20	30	27	33
	IC_{50} (nM ± standard deviation, $n \geq 3$)[b]											
iNOS	193 ± 38 (28)[c]	220 ± 25	685 ± 127	282 ± 49	1776 ± 395	>5000	>5000	57.6 ± 5.3	170 ± 26	731 ± 87	>5000	>5000
eNOS	(150)[c]	1500 ± 300	−*d*	–	–	–	–	1428 ± 158	–	–	–	–
nNOS	(100)[c]	490 ± 80	–	–	–	–	–	514 ± 83	–	–	–	–

[a] Using recombinant human iNOS, eNOS, and nNOS. [b] Standard iNOS IC_{50} [measured (reported)]: SEITU = 30.5 ± 4.6 (32), L-NIL = 1465 ± 148 (1400), 2-AP = 108 ± 35 (170). [c] Reference 10. [d] −: Not determined.

Table 2. Biodistribution of [^{18}F]**9** in Control vs LPS Treated Mice[a] (Data Reported as Mean %ID/g ± SD; $n = 4$)[b]

	5 min		30 min		1 h		2 h	
%ID/g	LPS	control	LPS	control	LPS	control	LPS	control
blood	3.69 ± 0.38	2.37 ± 0.18	2.09 ± 0.35	1.22 ± 0.16	0.86 ± 0.09	0.31 ± 0.04	0.23 ± 0.05	0.27 ± 0.22
lung	4.32 ± 0.32	3.33 ± 0.28	1.84 ± 0.27	1.14 ± 0.13	0.73 ± 0.17	0.31 ± 0.06	0.18 ± 0.09	0.15 ± 0.03
liver	24.6 ± 3.1	33.2 ± 3.3	7.06 ± 0.28	10.7 ± 0.3	2.63 ± 0.52	2.59 ± 0.49	0.42 ± 0.15	0.74 ± 0.23
kidney	26.7 ± 4.1	20.6 ± 2.4	10.9 ± 2.8	7.30 ± 0.66	3.95 ± 0.53	2.20 ± 0.25	0.91 ± 0.63	0.80 ± 0.27
muscle	1.64 ± 0.09	1.25 ± 0.06	1.06 ± 0.40	0.71 ± 0.31	0.78 ± 0.47	0.27 ± 0.18	0.23 ± 0.13	0.34 ± 0.27
heart	2.03 ± 0.06	1.50 ± 0.12	1.02 ± 0.16	0.60 ± 0.05	0.41 ± 0.10	0.19 ± 0.02	0.12 ± 0.04	0.08 ± 0.02
brain	1.81 ± 0.09	1.60 ± 0.17	0.52 ± 0.15	0.28 ± 0.02	0.19 ± 0.03	0.11 ± 0.02	0.07 ± 0.03	0.07 ± 0.03
bone	1.59 ± 0.15	1.52 ± 0.36	3.70 ± 1.20	2.26 ± 0.55	4.30 ± 0.90	2.57 ± 0.64	3.77 ± 1.41	5.59 ± 4.20

[a] LPS mice were treated with lipopolysaccharide (LPS) 10 mg/kg iv 6 h prior to tracer injection; all mice were injected with 50 μCi/110 μL [^{18}F]**9**. [b] SD: standard deviation.

atom (i.e., **9**), the potency for iNOS remained the same. Introduction of a double bond to **2** to give an alkene analogue, **24**, resulting in a diminished potency for iNOS. Removal of the *cis* methyl from **24** (i.e., **11**) regained the potency for iNOS (IC_{50} = 282 nM); this change in potency for iNOS from **24** and **11** implies that steric demand at the 6-position is high. The change from the methyl in **2** or fluorine in **9** to the hydroxy group in **16** resulted in a large reduction in potency for iNOS, suggesting an adverse electronic substituent effect in this position. The corresponding methoxy (i.e., **13**) and 2-fluoroethoxy (i.e., **15**) analogues were inactive. Compound **18**, an isomer of **9** with the fluorine at the terminal position, had enhanced potency and selectivity for iNOS; however, extension of the alkyl chain in **18** by one methylene group (i.e., **20**) resulted in a reduction of potency for iNOS. Addition of a methyl group in the 2′-position of **20** to give **30** resulted in a further decrease in potency for iNOS. The corresponding MeO or MeS analogues, **27** and **33**, were inactive in the iNOS assay. In summary, there appear to be significant steric and electronic constraints for substituents at the 6-position of the pyridine ring with respect to potency for inhibiting iNOS.

In Vitro Stability and in Vivo Metabolism Studies. An in vitro stability study was carried out using heparinized rat blood taken from an adult male Sprague−Dawley rat. [^{18}F]**9** was relatively stable in the whole blood for the duration of the experiment (2 h) at 37 °C. At 1 h, ~80% of the activity recovered from lysed whole blood was observed as [^{18}F]**9**, and at 2 h, ~75% of the recovered activity was still that of the parent compound. These data suggest that the blood is not a major site for compound degradation, which is in contrast to the previously reported ^{18}F and ^{11}C labeled isothiourea analogues.[12a]

The in vivo metabolic stability of [^{18}F]**9** was evaluated in plasma samples obtained from an adult male Sprague−Dawley rat at 5 and 30 min postinjection. The supernatant extracts were analyzed by silica gel radio-TLC and reversed-phase HPLC. After 30 min, the percent parent compound was only 20.2%. Additionally, within 5 min postinjection, only 40.3% of the activity in the blood was [^{18}F]**9**, which was confirmed by HPLC coelution with nonradioactive **9**. According to the HPLC analysis, the major metabolite, constituting 50% of the activity in blood at 5 min postinjection, was very polar but was not free [^{18}F]fluoride. This observation is also consistent with the low bone uptake reported below in the biodistribution studies (Table 2). Because [^{18}F]**9** demonstrated reasonable in vitro stability in whole blood, the metabolite observed in vivo at 5 min in blood must be due to metabolism in peripheral organs.

In Vivo Biodistribution Study. The biodistribution studies were performed in mature male C57BL/6 mice: one group was treated with bacterial lipopolysaccharide (LPS) (10 mg/kg, iv) to induce iNOS expression and one group was without LPS-treatment as control. LPS has been well documented to induce iNOS mRNA and protein expression in both rats and mice,[16] and administration of LPS resulted in an elevated iNOS expression at 6−7 h post-LPS-treatment. The iNOS distribution in organs was reported recently in male BALB/c mice.[16c] It has been demonstrated in that report that iNOS mRNA and protein expression 6 h after LPS stimulation is observed in many organs, including lungs, heart, liver, spleen, gut, and kidneys. Among them, the highest iNOS expression was in the lungs, with moderate expression in the spleen and kidneys and the lowest in the heart, gut, and liver.[16c] Therefore, this endotoxin (LPS) lung injury mouse model was used to assess the efficiency of [^{18}F]**9** as an iNOS radiotracer.

The results of in vivo biodistribution studies in the normal and LPS-treated mice are shown in Table 2 and Figure 1. The highest uptake in both groups was observed in the liver and kidneys, which are likely to be the major metabolic and/or excretory sites for the tracer. Excluding the potential metabolic sites, the highest uptake was observed in the lungs and blood, followed by muscle, heart, and brain in both groups. The low bone uptake suggested that [^{18}F]**9** had a high degree of stability toward defluorination, considering the facile elimination to form

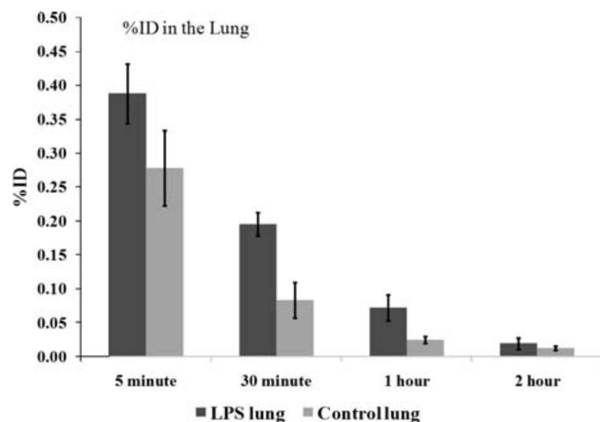

Figure 1. Comparison of total lung activity postinjection of [^{18}F]**9** in LPS-pretreated mice vs control mice.

a conjugated double bond at this position. Compared to the control group, the LPS-treated mice had a ~30% increase in tracer uptake in most of the organs at 1 h. In the organ expected to have the highest iNOS expression, the lungs, the increase in injected dose/g (ID/g) was even more pronounced, 30% at 5 min, 60% at 30 min, and 130% at 1 h. Because systemic LPS-induced acute lung injury results in pulmonary edema, the difference in total lung uptake between control and treated animals (i.e., %ID) is more dramatic than the %ID/g in the lung (Figure 1). The overall higher uptake in tissues of the LPS-treated mice compared to the controls is consistent with the previously reported systemic iNOS response with LPS treatment.[16c] From 30 min to 1 h, the uptake in the LPS-treated mice washed out at a slower rate than that of the control mice, which again can be attributed to the specific binding of [^{18}F]**9** to iNOS. On the basis of the in vivo metabolic stability study in the blood of normal rat (see above), there should be little circulating [^{18}F]**9** left in the blood of the mice at 2 h postinjection. At 2 h postinjection, all the activity was washed out to the same low level and the uptake at 2 h postinjection should be due to the nonspecific uptake of the metabolites. In previously reported biodistribution studies in rats injected with less potent and less selective ^{18}F and ^{11}C labeled isothiourea analogues, about 30% higher uptake of ^{18}F labeled analogue was observed in lungs, blood, liver, kidneys, and heart of LPS-treated rats than that of normal rats at 10 min postinjection. However, the difference in uptake between the two groups became insignificant at 30 min postinjection, possibly due to the rapid metabolism of these radiotracers. The more stable ^{11}C labeled analogue showed 40% higher uptake at 30 min postinjection in the lungs of the LPS-treated rats than that of the control.[12a] Compared to the previously described ^{18}F labeled isothiourea analogue, [^{18}F]**9**, with prolonged retention in the LPS-treated mice, is a suitable PET tracer for iNOS.

A standard Western blot was performed to compare the iNOS induction in lungs upon LPS stimulation versus untreated controls, and the results are shown in Figure 2. Protein for the Western blot was obtained from the lungs harvested from treated and untreated animals in the biodistribution study. The first lane is the purified iNOS protein as a positive control. Protein from two control lungs and six LPS-treated lungs were evaluated. As indicated in Figure 2, neither of the control samples demonstrated iNOS expression, whereas the LPS-treated samples all showed some degree of iNOS induction due to the response toward LPS stimulation. This result is consistent with the higher

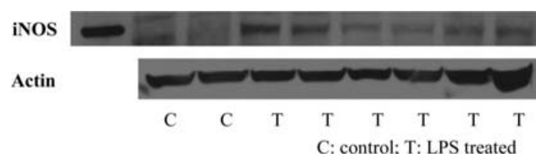

Figure 2. Representative Western blots showing the levels of iNOS expression in lungs from the control and LPS treated mice. The first lane is purified iNOS as a positive control (iNOS); no iNOS expression was observed in the lungs of normal mice (C); different degrees of iNOS expression were found in the lungs of the LPS-treated mice (T).

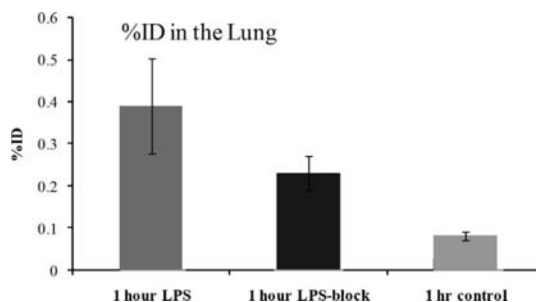

Figure 3. Comparison of activity in the lung 1 h postinjection of [^{18}F]**9** in the control, LPS treated, and LPS-treated-1400W-blocked mice (mean %ID/g ± SD, $n = 4$, $p < 0.05$).

tracer uptake in the lungs of the LPS-treated mice in the biodistribution studies, suggesting iNOS-specific uptake of [^{18}F]**9**.

Blocking Study. To further demonstrate that the increased uptake in the LPS-treated mice was due to specific binding of [^{18}F]**9** to iNOS, blocking studies were carried out. First, the nonselective NOS inhibitor 2-amino-4-methylpyridine (**1**) (10 mg/kg, iv) failed to block the increased uptake in the LPS-treated mice (data not shown). A failure to block tracer uptake using nonselective NOS inhibitors *S*-methyl or *S*-ethyl isothiourea has been reported previously;[12a] the failure was contributed to the blood pressure change caused by the blocking agents in the animal, which may alter the tracer uptake function. 2-Amino-4-methylpyridine (**1**) elevates blood pressure[9a,10,17] and blocking of eNOS expression may also reduce the blood flow.[18] Therefore, a highly selectively iNOS inhibitor is preferred in order to avoid the side effects from nonselective inhibitors. *N*-(3-(Aminomethyl)benzyl)acetamidine (1400W) is a slow, tight binding, and highly selective inhibitor of iNOS in vitro and in vivo[8b] and has been used commonly as an iNOS inhibitor in many reported studies. However, due to its high toxicity,[19] only 5 mg/kg of 1400W was injected intravenously immediately before the injection of [^{18}F]**9**. The results are shown in Figure 3. At 1 h post injection of [^{18}F]**9**, 32% of the tracer uptake in the lungs and blood of the LPS-treated mice was blocked by 1400W (Figure 3). This reduced uptake in the lungs of the LPS-treated mice should be due to the specific blocking of iNOS by 1400W and is consistent with that the uptake of [^{18}F]**9** in the LPS-treated mice is iNOS specific.

MicroPET Study. A microPET imaging study using [^{18}F]**9** was carried out on an intratracheally LPS-treated mouse and a normal mouse as control. The microPET images (0−60 min dynamic scan) are shown in Figure 4. As shown in the microPET images (Figure 4), accumulation of [^{18}F]**9** was observed in the target organ, the lungs, of the LPS-treated mouse, whereas no such accumulation was observed in the lungs of the normal mouse. The difference in the tracer uptake in the lungs of the LPS-treated and control mice is consistent with

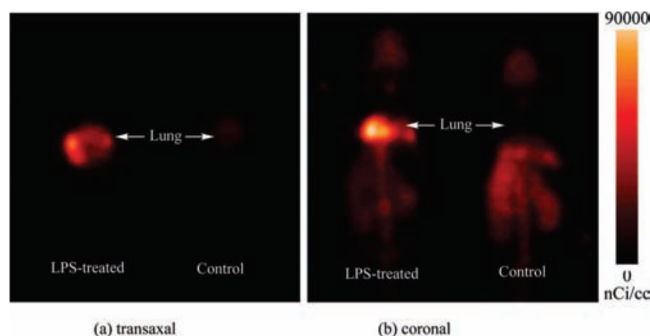

Figure 4. Whole-body MicroPET images of [^{18}F]**9** in the LPS-treated mice (left) and the control mice (right): (a) transaxal, (b) coronal. Images were summed from 0 to 60 min after injection of [^{18}F]**9**. Accumulation of the activity was observed in the lungs of the LPS-treated mouse, whereas there is no such accumulation in the normal control.

iNOS expression induced by LPS treatment and is similar to the results of biodistribution study.

Conclusion

We have identified 6-(2-fluoropropyl)-4-methylpyridin-2-amine (**9**), 6-(3-fluoropropyl)-4-methylpyridin-2-amine (**18**), and 6-(4-fluorobutyl)-4-methylpyridin-2-amine (**20**) as iNOS inhibitors with the greatest potential to serve as PET radiotracers. [^{18}F]**9** was synthesized in modest yield (~10%) but with high chemical and radiochemical purities. In the biodistribution study of a mouse model of LPS-induced iNOS activation, higher uptake of [^{18}F]**9** was observed in the lungs of the LPS-treated mice than those in the control mice. The higher uptake in the lungs of the LPS-treated animals correlated well with iNOS expression, which was confirmed by Western blot analysis of the lung samples from control and LPS-treated mice. The increased uptake in the lungs of the LPS-treated mice at 60 min post injection of [^{18}F]**9** was reduced by injection of the highly selective iNOS inhibitor, 1400W. The blocking study suggests that the higher uptake of [^{18}F]**9** in the lungs of the LPS-treated mice is due to specific binding of [^{18}F]**9** to iNOS. MicroPET study of the LPS-treated mouse using [^{18}F]**9** demonstrated an accumulation of [^{18}F]**9** in the lungs of the LPS-treated mice, in sharp contrast to those of the control mouse. In conclusion, [^{18}F]6-(2-Fluoropropyl)-4-methylpyridin-2-amine ([^{18}F]**9**) is a potential radiotracer for PET imaging of iNOS expression.

Experimental Section

General Methods and Materials. All chemicals were obtained from standard commercial sources and used without further purification. All reactions were carried out by standard air-free and moisture-free techniques under an inert argon atmosphere with dry solvents unless otherwise stated. Flash column chromatography was conducted using Scientific Adsorbents, Inc. silica gel, 60A, "40 Micron Flash" (32−63 μm). Melting points were uncorrected. Routine ^{1}H NMR spectra were recorded at 300 MHz. All chemical shifts were reported as a part per million (ppm) downfield from tetramethylsilane (TMS) or when chloroform-*d* was used as solvent and the solvent peak at δ 7.25 ppm was used as an internal standard. All coupling constants (*J*) are given in Hz. Splitting patterns are typically described as follows: s, singlet; d, doublet; t, triplet; m, multiplet. ^{19}F NMR spectra were recorded at 282.2 MHz, and chemical shifts are reported as Hz upfield from an external $CFCl_3$ standard. ESI/MS was performed on a Waters ZQ 4000 single quadrupole mass spectrometer equipped with an electrospray ionization (ESI) LC-MS interface. High-performance liquid chromatography (HPLC) was performed with an ultraviolet detector operating at 272 nm and a well-scintillation NaI (Tl) detector and associated electronics for radioactivity detection. Alltech Platinum EPS C18 250 mm × 10 mm semipreparative column and Alltech Platinum EPS C18 250 mm × 4.6 mm analytical column were used for preparation and analysis, respectively. 4-Methoxybutan-2-one was synthesized according to literature.[20] The purities of final compounds are ≥95%, which were confirmed by examination of elemental analysis results or by reversed-phase HPLC (for compound **13**, **15**, **18**, **24**, and **27**).

$H_2{}^{18}O$ was purchased from Rotem Industries (Israel). [^{18}F]Fluoride was produced in Washington University by the $^{18}O(p,n)^{18}F$ reaction through proton irradiation of enriched (95%) ^{18}O water using a RDS111 cyclotron. Materials were heated using a custom-designed microwave cavity, model 420BX (Micro-Now Instruments, Skokie, IL). Screw-cap test tubes used for microwave heating were purchased from Fisher Scientific (Pyrex no. 9825). HLB Sep-Pak cartridges were purchased from Waters Corporation. For the TLC analyses, EM Science Silica Gel 60 F_{254} TLC plates were purchased from Fisher Scientific (Pittsburgh, PA). Radio-TLC was accomplished using a Bioscan 200 imaging scanner (Bioscan, Inc., Washington, DC). Radioactivity was counted with a Beckman Gamma 8000 counter containing a NaI crystal (Beckman Instruments, Inc., Irvine, CA).

Typical Procedure for the Synthesis of 6. Into a solution of **5** (2.0 g, 10 mmol) in dry Et_2O (20 mL) at −20 °C was added dropwise *n*-BuLi (1.6 M in hexane, 6.9 mL, 10 mmol) within 5 min, then the reaction mixture was stirred at −20 to −10 °C for 1 h to complete the reaction. Orange solids precipitated gradually during the experiment, and the reaction mixture of **6** was used directly for further reactions.

1-(6-(2,5-Dimethyl-1*H*-pyrrol-1-yl)-4-methylpyridin-2-yl)propan-2-ol (7). Into an Et_2O solution of **6** at −78 °C, which was made from **5** (5.6 g, 28.0 mmol), *n*-BuLi (1.6 M in hexane, 19.5 mL, 31.2 mmol) in Et_2O (30 mL) was added CH_3CHO (2 mL, 35.6 mmol) via a syringe. The reaction mixture was allowed to warm up to room temperature, and stirring was continued for 10 min. Then, the reaction mixture was treated with H_2O (100 mL) and extracted with ethyl acetate (3 × 50 mL). The organic solution was washed with brine (2 × 30 mL), dried over $NaSO_4$, and the solvent was evaporated under reduced pressure. The crude product was purified with silica gel chromatograph using 1:4 ethyl acetate/hexanes to afford **7** (5.6 g) in 80% yield as colorless liquid. ^{1}H NMR (CD_3Cl, 300 MHz) δ 6.97 (s, 1H), 6.89 (s, 1H), 5.87 (s, 2H), 4.51 (s, br, 1H), 4.23 (m, 1H), 2.94−2.80 (m, 2H), 2.39 (s, 3H), 2.12 (s, 6H), 1.25 (d, 3H, $J = 6.3$ Hz).

2-(2,5-Dimethyl-1*H*-pyrrol-1-yl)-6-(2-fluoropropyl)-4-methylpyridine (8). Using Diethylaminosulfur Trifluoride (DAST) as Fluorinating Agent. Into a solution of **7** (0.5 g, 2.05 mmol) in CH_2Cl_2 (5 mL) at 0 °C was added DAST (0.4 mL, 3.05 mmol) dropwise. The reaction mixture became brown in color, and the starting material was consumed within 30 min. Saturated $NaHCO_3$ solution (10 mL) was added to quench the reaction, and the aqueous solution was extracted with ethyl acetate (2 × 30 mL). The organic layers was washed with brine (2 × 30 mL) and dried over Na_2SO_4. Solvents were evaporated under reduced pressure, and the crude product was purified with silica gel chromatograph using 1:10 ethyl acetate/hexanes to afford **8** (0.13 g) in 26% yield as colorless liquid. ^{1}H NMR (CD_3Cl, 300 MHz) δ 7.08 (s, 1H), 6.93 (s, 1H), 5.91 (s, 2H), 5.05−5.60 (m, 1H), 3.20 (m, 2H), 2.43 (s, 3H), 2.15 (s, 6H), 1.43 (dd, 3H, $J = 23.4$, 6.3 Hz), ESI/MS *m/z* 247.06 [M + H$^+$].

Using Perfluorobutane Sulfonyl Fluoride (PBSF) as Fluorinating Agent. Into a solution of **7** (0.5 g, 2.05 mmol) in CH_3CN (5 mL) were added PBSF (0.74 mL, 4.1 mmol), Et_3N (1.73 mL, 12.4 mmol), and $(NEt_3)(HF)_3$ (0.67 mL, 4.11 mmol). The reaction mixture was stirred quickly and became homogeneous after 40 min. The reaction was completed in 2.5 h according to TLC analysis, and the solvent was evaporated under reduced pressure. Silica gel chromatograph purification of the residue using 1:10 ethyl acetate/hexanes afforded **8** (0.13 g) in 26% yield as colorless liquid.

6-(2-Fluoropropyl)-4-methylpyridin-2-amine (9): Typical Procedure for Deprotection. Into a 50 mL round-bottom flask equipped with a magnetic stirring bar and a condenser were added

8 (1.10 g, 4.1 mmol) and $NH_2OH \cdot HCl$ (10 g, 144 mmol), followed by ethanol (25 mL) and water (12.5 mL). The reaction mixture was stirred at reflux and the progress was monitored by TLC. Upon the completion of the reaction, in about 3 h, the reaction mixture was treated with saturated Na_2CO_3 solution (10 mL) and extracted with CH_2Cl_2 (3 × 20 mL). The combined organic layers was washed with brine (2 × 20 mL) and dried over Na_2SO_4. After removal of volatiles under reduced pressure, the crude product was purified with silica gel chromatograph using ethyl acetate to afford **9** (0.61 g) in 81% yield as light-yellow solid (mp 51.0−52.5 °C; oxalate 154.0−155.9 °C). The oxalate was precipitated using 1:1 of **9** and oxalic acid in ethyl acetate to afford the salt as a white solid. ^{1}H NMR (CD_3Cl, 300 MHz) δ 6.40 (s, 1H), 6.18 (s, 1H), 5.20−4.90 (m, 1H), 4.37 (s, br, 2H), 3.00−2.70 (m, 2H), 2.19 (s, 3H), 1.37 (dd, 3H, J = 24.0, 6.3 Hz).

***(E)*-2-(2,5-Dimethyl-1*H*-pyrrol-1-yl)-4-methyl-6-(prop-1-enyl)pyridine (10).** Compound **10** was obtained as a byproduct during the synthesis of **9** using PBSF as fluorinating agent in 49% yield as colorless liquid. ^{1}H NMR (CD_3Cl, 300 MHz) δ 7.00 (s, 1H), 6.83 (s, 1H), 6.85−6.78 (m, 1H), 6.51−6.44 (s, 1H), 5.88 (s, 2H), 2.38 (s, 3H), 2.15 (s, 6H), 1.92 (d, 3H, J = 6.9 Hz).

***(E)*-4-Methyl-6-(prop-1-enyl)pyridin-2-amine (11).** Compound **11** was synthesized from **10** using the standard deprotection procedure in 53% yield as a solid (mp 66.4−67.0 °C; oxalate 137.5−138.7 °C)). ^{1}H NMR (CD_3Cl, 300 MHz) δ 6.67−6.56 (m, 1H), 6.40 (s, 1H), 6.28 (d, 1H, J = 15.3 Hz), 6.14 (s, 1H), 4.42 (s, br, 2H), 2.17 (s, 3H), 1.86 (d, 3H, J = 7.2 Hz).

2-(2,5-Dimethyl-1*H*-pyrrol-1-yl)-6-(2-methoxypropyl)-4-methylpyridine (12). Into a solution of **7** (0.9 g, 3.68 mmol) in freshly distilled THF (20 mL) was added 60% NaH in mineral oil (0.3 g, 12.6 mmol). After 5 min, MeI (0.5 mL, 8.03 mmol) was added and the reaction mixture was stirred at room temperature for 5 h. The mixture was then quenched with an aqueous 1 N HCl solution, followed by neutralization with saturated solution of aqueous Na_2CO_3. The product was extracted with ethyl acetate (3 × 20 mL), and the combined organic layers were washed with brine (30 mL) and dried over $MgSO_4$. After evaporation of solvents under reduced pressure, silica gel chromatograph purification of the residue using 1:4 ethyl acetate/hexanes afforded **12** (0.89 g) in 94% yield as a light-yellow liquid. ^{1}H NMR (CD_3Cl, 300 MHz) δ 7.01 (s, 1H), 6.86 (s, 1H), 5.87 (s, 2H), 3.84 (m, 1H), 3.30 (s, 3H), 3.05−2.70 (m, 2H), 2.39 (s, 3H), 2.11 (s, 6H), 1.17 (d, 3H, J = 6.0 Hz).

6-(2-Methoxypropyl)-4-methylpyridin-2-amine (13). Compound **13** was synthesized from **12** using the standard deprotection method. The corresponding oxalate was precipitated using 1:1 of **13** and oxalic acid in ethyl acetate to afford the salt as a white solid (mp oxalate 123−125 °C). ^{1}H NMR (CD_3Cl, 300 MHz) δ 6.35 (s, 1H), 6.13 (s, 1H), 4.49 (s, br, 2H), 3.71 (m, 1H), 3.30 (s, 3H), 2.89−2.49 (m, 2H), 2.16 (s, 3H), 1.12 (d, 3H, J = 6 Hz).

2-(2,5-Dimethyl-1*H*-pyrrol-1-yl)-6-(2-(2-fluoroethoxy)propyl)-4-methylpyridine (14). Into a solution of **7** (1.0 g, 4.1 mmol) in freshly distilled THF (20 mL) were added 60% NaH in mineral oil (0.35 g, 8.8 mmol) and 1-bromo-2-fluoroethane (1.0 mL, 8 mmol). The reaction mixture was stirred at room temperature for 6 h and then at 60 °C overnight. The reaction mixture was filtered, and the organic solution was washed with 1 N HCl solution, saturated Na_2CO_3, and brine and then dried over Na_2SO_4. Solvent was evaporated under reduced pressure, and the residue was purified by silica gel chromatograph using 1:8 ethyl acetate/hexanes to afford **14** (0.37 g) in 31% yield as colorless liquid. ^{1}H NMR (CD_3Cl, 300 MHz) δ 7.04 (s, 1H), 6.86 (s, 1H), 5.87 (s, 2H), 4.54−4.35 (m, 2H), 3.97 (m, 1H), 3.79−3.53 (m, 2H), 3.09−2.81 (m, 2H), 2.38 (s, 3H), 2.10 (s, 6H), 1.20 (d, 3H, J = 6.3 Hz).

6-(2-(2-Fluoroethoxy)propyl)-4-methylpyridin-2-amine (15). Compound **15** was synthesized from **14** using the standard deprotection procedure in 81% yield as solid (mp 60.2−63.0 °C; oxalate 163−164 °C). ^{1}H NMR (CD_3Cl, 300 MHz) δ 6.40 (s, 1H), 6.16 (s, 1H), 4.56−4.37 (m, 2H), 4.35 (s, br, 2H), 3.88 (m, 1H), 3.67−3.53 (m, 2H), 2.92−2.55 (m, 2H), 2.18 (s, 3H), 1.18 (d, 3H, J = 6.3 Hz).

1-(6-Amino-4-methylpyridin-2-yl)propan-2-ol (16). Compound **16** was synthesized from **7** using the standard deprotection procedure in 66% yield as a light-yellow solid (mp 95−96 °C). ^{1}H NMR (CD_3Cl, 300 MHz) δ 6.31 (s, 1H), 6.18 (s, 1H), 4.30 (s, br, 1H), 4.12 (m, 1H), 2.62 (m, 2H), 2.19 (s, 3H), 1.23 (d, 3H, J = 6.0 Hz).

2-(2,5-Dimethyl-1*H*-pyrrol-1-yl)-6-(3-fluoropropyl)-4-methylpyridine (17). Into an Et_2O solution of **5** at −78 °C, which was made from **3** (2.0 g, 10 mmol), *n*-BuLi (1.6 M in Hexane, 8.0 mL, 12.8 mmol)) in Et_2O (20 mL), was added $BrCH_2CH_2F$ (2 0.0 g, 15.7 mmol) via a syringe. The reaction mixture was allowed to warm up to room temperature and continued to stir for 30 min. Then the reaction mixture was treated with saturated Na_2CO_3 solution and then brine. The organic solution was dried over Na_2SO_4, and the solvent was evaporated under reduced pressure. The crude product was purified with silica gel chromatograph using 1:8 ethyl acetate/hexanes to afford **29** (1.6 g) in 61% yield as colorless liquid. ^{1}H NMR (CD_3Cl, 300 MHz) δ 7.04 (s, 1H), 6.91 (s, 1H), 5.92 (s, 2H), 4.53 (dt, 2H, J = 6.0, 47.4 Hz), 2.95 (t, 2H, J = 7.5 Hz), 2.44 (s, 3H), 2.3−2.1 (m, 2H), 2.16 (s, 6H). ^{19}F NMR (CD_3Cl, 282.2 MHz) δ −42.9.

6-(3-Fluoropropyl)-4-methylpyridin-2-amine (18). **18** was synthesized from **17** using the standard deprotection procedure in 55% yield as light-yellow solid (mp oxalate 112 °C decomposition). ^{1}H NMR (CD_3Cl, 300 MHz) δ 6.35 (s, 1H), 6.14 (s, 1H), 4.45 (dt, 2H, J = 6.0, 47.1 Hz), 4.37 (s, br, 2H), 2.66 (t, 2H, J = 7.6 Hz), 2.18 (s, 3H), 2.20−2.00 (m, 2H). ^{19}F NMR (CD_3Cl, 282.2 MHz) δ −42.6.

2-(2,5-Dimethyl-1*H*-pyrrol-1-yl)-6-(4-fluorobutyl)-4-methylpyridine (19). Into an Et_2O solution of **6** at −78 °C, which was made from **5** (3.0 g, 15 mmol) and *n*-BuLi (1.6 M in hexane, 11.0 mL, 17.6 mmol)) in Et_2O (30 mL), was added $BrCH_2CH_2CH_2CH_2F$ (2.1 g, 15.0 mmol) via a syringe. The reaction mixture was allowed to warm up to room temperature and continued to stir for 30 min. The reaction mixture was then treated with saturated Na_2CO_3 solution and brine. The organic was dried over $NaSO_4$, and the solvent was evaporated under reduced pressure. The crude product was purified with silica gel chromatograph using 1:10 ethyl acetate/hexanes to afford **19** (2.5 g) in 63% yield as colorless liquid. ^{1}H NMR (CD_3Cl, 300 MHz) δ 6.98 (s, 1H), 6.85 (s, 1H), 5.87 (s, 2H), 4.47 (dt, 2H, J = 6.0, 47.1 Hz), 2.82 (t, 2H, J = 7.5 Hz), 2.39 (s, 3H), 2.11 (s, 6H), 1.9−1.7 (m, 4H). ^{19}F NMR (CD_3Cl, 282.2 MHz) δ −41.7.

6-(4-Fluorobutyl)-4-methylpyridin-2-amine (20). Compound **20** was synthesized from **19** using the standard deprotection procedure in 57% yield as light-yellow solid (mp oxalate 133.0−135.0 °C). ^{1}H NMR (CD_3Cl, 300 MHz) δ 6.33 (s, 1H), 6.14 (s, 1H), 4.44 (dt, 2H, J = 6.0, 47.4 Hz), 4.38 (s, br, 2H), 2.58 (t, 2H, J = 7.4 Hz), 2.18 (s, 3H), 1.8−1.65 (m, 4H). ^{19}F NMR (CD_3Cl, 282.2 MHz) δ −41.5.

2-(2,5-Dimethyl-1*H*-pyrrol-1-yl)-4-methyl-6-((trimethylsilyl)-methyl)pyridine (21). Into an Et_2O solution of **6** at −78 °C, which was made from **5** (5.78 g, 28.9 mmol) and *n*-BuLi (1.6 M in Hexane, 21.6 mL, 34.6 mmol) in Et_2O (50 mL), was added Me_3SiCl (4.4 mL, 34.6 mmol) via a syringe. The reaction mixture was allowed to warm up to room temperature and continued to stir for 30 min. Then the reaction mixture was treated with saturated Na_2CO_3 solution and washed with brine. The organic solution was dried over $NaSO_4$, and the solvent was evaporated under reduced pressure. The crude product was purified with silica gel chromatograph using 1:4 ethyl acetate/hexanes to afford **21** (7.4 g) in 94% yield as colorless liquid. ^{1}H NMR (CD_3Cl, 300 MHz) δ 6.79 (s, 1H), 6.72 (s, 1H), 5.84 (s, 2H), 2.35 (s, 2H), 2.07 (s, 6H), 0.03 (s, 9H). ESI/Ms: m/z 273.2 ($M + H^+$).

2-(2,5-Dimethyl-1*H*-pyrrol-1-yl)-4-methyl-6-(2-methylprop-1-enyl)pyridine (23). Into a solution of **21** (1.0 g, 3.67 mmol) in Et_2O (10 mL) at −20 °C was added dropwise *n*-butyl lithium (1.6 M in hexane, 2.75 mL, 4.4 mmol). The reaction solution turned brown in color and was stirred at −20 to −10 °C for 2 h to afford a solution of ((6-(2,5-dimethyl-1*H*-pyrrol-1-yl)-4-methylpyridin-2-yl)(trimethylsilyl)methyl)lithium (**22**). The solution was then cooled

to −78 °C, and 2 mL of acetone was added. The solution became clear in slightly yellow color, and it was allowed to warm up to room temperature during 20 min. The organic solution was acidified with 1 N HCl (6 mL), followed by washing with saturated Na_2CO_3 solution, brine, and dried over Na_2SO_4. Solvent was evaporated under reduced pressure, and the crude product was purified with silica gel chromatograph using 1:15 ethyl acetate/hexanes to afford **23** (0.56 g) in 64% yield as colorless liquid. ^{1}H NMR (CD_3Cl, 300 MHz) δ 6.97 (s, 1H), 6.79 (s, 1H), 6.28 (s, 1H), 5.86 (s, 2H), 2.38 (s, 3H), 2.13 (s, 6H), 2.12 (s, 3H), 1.94 (s, 3H). ESI/MS: *m/z* 241.2 (M + H$^+$).

4-Methyl-6-(2-methylprop-1-enyl)pyridin-2-amine (24). Compound **24** was synthesized from **23** using the standard deprotection procedure in 64% yield as slightly yellow liquid (mp oxalate 154−156 °C). ^{1}H NMR (CD_3Cl, 300 MHz) δ 6.38 (s, 1H), 6.13 (s, 1H), 6.12 (s, 1H), 4.37 (s, br, 2H), 2.17 (s, 3H), 1.99 (s, 3H), 1.87 (s, 3H).

(*E*/*Z*)2-(2,5-Dimethyl-1*H*-pyrrol-1-yl)-6-(4-methoxy-2-methylbut-1-enyl)-4-methylpyridine (25). Into an Et_2O solution of **22** at −78 °C, which was made from **21** (1.0 g, 3.67 mmol) and *n*-BuLi (1.6 M in hexane, 2.75 mL, 4.4 mmol) in Et_2O (10 mL), was added 4-methoxybutan-2-one (0.45 g, 4.4 mmol). After the addition, the reaction mixture was allowed to warm up to room temperature during 30 min. The mixture was then acidified with 1 N HCl (6 mL), neutralized by saturated Na_2CO_3 solution, and diluted with ethyl acetate (50 mL). The organic solution was washed with brine and dried over Na_2SO_4. Solvent was evaporated under reduced pressure, and the crude product was purified with silica gel chromatograph using 1:15 and 1:8 ethyl acetate/hexanes to afford *E* and *Z* isomers of **23** (0.25 and 0.22 g) in 45% total yield as colorless liquid. ^{1}H NMR (CD_3Cl, 300 MHz) δ 7.01 (s, 1H), 6.81 (s, 1H), 6.35 (s, 1H), 5.85 (s, 2H), 3.55 (t, 2H, *J* = 7.2 Hz), 3.25 (s, 3H), 2.90 (t, 2H, *J* = 7.2 Hz), 2.38 (s, 3H), 2.11 (s, 6H), 1.97 (s, 3H) and δ 7.00 (s, 1H), 6.80 (s, 1H), 6.33 (s, 1H), 5.87 (s, 2H), 3.58 (t, 2H, *J* = 6.6 Hz), 3.37 (s, 3H), 2.48 (t, 2H, *J* = 6.90 Hz), 2.38 (s, 3H), 2.16 (s, 3H), 2.13 (s, 6H).

2-(2,5-Dimethyl-1*H*-pyrrol-1-yl)-6-(4-methoxy-2-methylbutyl)-4-methylpyridine (26). Into a 100 mL round-bottom flask equipped with a magnetic stirring bar were loaded the isomeric mixture of **25** (0.47 g, 1.7 mmol) and absolute EtOH (20 mL), followed by 10% Pd/C (0.25 g). The reaction mixture was stirred in an 80 °C oil bath, and the reaction was completed in 1 h according to TLC analysis. Solids were removed by filtration and solvent was evaporated under reduced pressure. The residue was dissolved in ethyl acetate, and the organic solution was treated with saturated Na_2CO_3 solution (10 mL) and washed with brine and dried over $MgSO_4$. Solvent was evaporated under reduced pressure, and the crude product was purified with silica gel chromatograph using 1:10 and 1:4 ethyl acetate/hexanes to afford **26** (0.38 g) in 81% yield as colorless liquid. ^{1}H NMR (CD_3Cl, 300 MHz) δ 6.94 (s, 1H), 6.83 (s, 1H), 5.86 (s, 2H), 3.41 (m, 2H), 3.30 (s, 3H), 2.82−2.55 (m, 2H), 2.37 (s, 3H), 2.15 (m, 1H), 2.10 (s, 6H), 1.69−1.44 (m, 2H), 0.90 (d, 3H, *J* = 6.60 Hz).

Synthesis of 6-(4-Methoxy-2-methylbutyl)-4-methylpyridin-2-amine (27). Compound **27** was synthesized from **26** using the standard deprotection procedure in 71% yield as slightly yellow solid (mp 48.0−50.0 °C). ^{1}H NMR (CD_3Cl, 300 MHz) δ 6.32 (s, 1H), 6.14 (s, 1H), 4.35 (s, br, 2H), 3.42 (m, 2H), 3.30 (s, 3H), 2.59−2.33 (m, 2H), 2.18 (s, 3H), 2.05 (m, 1H), 1.70−1.40 (m, 2H), 0.89 (d, 3H, *J* = 6.90 Hz).

(*E*/*Z*)-2-(2,5-Dimethyl-1*H*-pyrrol-1-yl)-6-(4-fluoro-2-methylbut-1-enyl)-4-methylpyridine (28). Compound **28** was synthesized from **22** and 4-fluorobutan-2-one using the method for **25** in 50% yield as a colorless liquid. ^{1}H NMR (CD_3Cl, 300 MHz) δ 6.97 (s, 1H), 6.79 (s, 1H), 6.38 (s, 1H), 4.61 (dt, 2H, *J* = 6.0, 47.1 Hz), 2.60 (dt, 2H, *J* = 6.1, 24.0 Hz), 2.38 (s, 3H), 2.10 (s, 6H), 2.00 (s, 3H) and δ 7.01 (s, 1H), 6.82 (s, 1H), 6.36 (s, 1H), 4.63 (dt, 2H, *J* = 6.3, 47.1 Hz), 3.09 (dt, 2H, *J* = 6.1, 25.2 Hz), 2.39 (s, 3H), 2.18 (s, 3H), 2.13 (s, 6H).

2-(2,5-Dimethyl-1*H*-pyrrol-1-yl)-6-(4-fluoro-2-methylbutyl)-4-methylpyridine (29). Compound **29** was synthesized from a mixture of **28** using ammonium formate in the presence of 10% Pd/C in 30% yield as colorless liquid. ^{1}H NMR (CD_3Cl, 300 MHz) δ 6.95 (s, 1H), 6.85 (s, 1H), 5.86 (s, 2H), 4.50 (dt, 2H, *J* = 6.0, 47.4 Hz), 2.83−2.59 (m, 2H), 2.38 (s, 3H), 2.28−2.18 (m, 1H), 2.06 (s, 6H), 1.87−1.48 (m, 2H), 0.93 (d, 3H, *J* = 6.9 Hz).

6-(4-Fluoro-2-methylbutyl)-4-methylpyridin-2-amine (30). Compound **30** was synthesized from **29** using the standard deprotection procedure in 47% yield as light-yellow solid (oxalate: mp 136.6−137.1 °C). ^{1}H NMR (CD_3Cl, 300 MHz) δ 6.31 (s, 1H), 6.15 (s, 1H), 4.67 (s, br, 2H), 4.50 (dt, 2H, *J* = 6.3, 47.4 Hz), 2.61−2.37 (m, 2H), 2.19 (s, 3H), 2.15−2.05 (m, 1H), 1.90−1.45 (m, 2H), 0.93 (d, 3H, *J* = 6.3 Hz). ^{19}F NMR (CD_3Cl, 282.2 MHz) δ −41.1.

(*E*/*Z*)-2-(2,5-Dimethyl-1*H*-pyrrol-1-yl)-4-methyl-6-(2-methyl-4-(methylthio)but-1-enyl)pyridine (31). Into an Et_2O solution of **22** at −78 °C, which was made from **21** (1.6 g, 5.87 mmol) and *n*-BuLi (1.6 M in hexane, 4.8 mL, 7.68 mmol) in Et_2O (25 mL), was added 4-(methylthio)butan-2-one (0.90 g, 7.61 mmol). The reaction mixture was allowed to warm to room temperature over 30 min. The reaction solution was then acidified with 1 N HCl (10 mL), followed by neutralization by saturated Na_2CO_3 solution. The mixture was diluted with ethyl acetate (50 mL), and the organic solution was washed with brine and dried over Na_2SO_4. Solvent was evaporated under reduced pressure, and the crude product was purified with silica gel chromatograph using 1:10 ethyl acetate/hexanes to afford *E*/*Z* isomer mixture of **31** (1.38 g) in 78% yield as colorless liquid. ^{1}H NMR (CD_3Cl, 300 MHz) δ 6.94 (s, 1H), 6.80 (s, 1H), 6.28 (d, 1H, *J* = 1.5 Hz), 5.83 (s, 2H), 2.90 (m, 2H), 2.62 (m, 2H), 2.37 (s, 3H), 2.09 (s, 6H), 1.95 (d, 3H, *J* = 1.5 Hz), 1.87 (s, 3H) and δ 7.00 (s, 1H), 6.80 (s, 1H), 6.32 (d, 1H, *J* = 1.2 Hz), 5.86 (s, 2H), 2.70 (m, 2H), 2.48 (m, 2H), 2.38 (s, 3H), 2.14 (s, 3H), 2.14 (d, 3H, *J* = 1.2 Hz), 2.12 (s, 6H).

2-(2,5-Dimethyl-1*H*-pyrrol-1-yl)-4-methyl-6-(2-methyl-4-(methylthio)butyl)pyridine (32). Into a solution of **31** (1.38 g, 4.6 mmol) in EtOH (30 mL) at 0 °C was added Mg turnings (1.25 g, 51 mmol). The reaction mixture was stirred at 0 °C for 1 h and then at room temperature overnight. All Mg turnings were consumed. The reaction mixture was acidified with 1 N HCl and then treated with saturated Na_2CO_3 solution and extracted with ethyl acetate (3 × 150 mL). The organic layers were combined, and the solvent was evaporated under reduced pressure. The residue was purified with silica gel chromatograph using 1:10 ethyl acetate/hexanes to afford **32** (0.42 g) in 30% yield as colorless liquid. ^{1}H NMR (CD_3Cl, 300 MHz) δ 6.97 (s, 1H), 6.86 (s, 1H), 5.88 (s, 2H), 2.80−2.50 (m, 4H), 2.40 (s, 3H), 2.15 (m, 1H), 2.12 (s, 6H), 2.07 (s, 3H), 1.7−1.5 (m, 2H), 0.92 (d, 3H, *J* = 6.90 Hz).

4-Methyl-6-(2-methyl-4-(methylthio)butyl)pyridin-2-amine (33). Compound **33** was synthesized from **32** using the standard deprotection procedure in 84% yield as a light-yellow solid (oxalate, mp 103.0−103.5 °C). ^{1}H NMR (CD_3Cl, 300 MHz) δ 6.32 (s, 1H), 6.15 (s, 1H), 4.62 (s, br, 2H), 2.62−2.34 (m, 4H), 2.20 (s, 3H), 2.08 (s, 3H), 2.04 (m, 1H), 1.75−1.42 (m, 2H), 0.90 (d, 3H, *J* = 6.6 Hz).

1-(6-(2,5-Dimethyl-1*H*-pyrrol-1-yl)-4-methylpyridin-2-yl)propan-2-yl acetate (34). Method 1. Into a solution of **7** (1.1 g, 4.50 mmol) in CH_2Cl_2 (20 mL) were added triethyl amine (0.94 mL, 6.75 mmol) and acetyl chloride (0.48 mL, 6.79 mmol). A white solid was formed instantly, and the reaction was stopped at 10 min by addition of methanol (1 mL). The reaction mixture was treated with saturated $NaHCO_3$ solution, and the product was extracted with CH_2Cl_2 (2 × 50 mL) and dried over Na_2SO_4. Solvent was removed under reduced pressure, and the residue was purified by silica gel chromatograph using 1:4 ethyl acetate/hexanes to afford **34** (0.5 g) in 39% yield as colorless liquid. ^{1}H NMR (CD_3Cl, 300 MHz) δ 7.00 (s, 1H), 6.89 (s, 1H), 5.87 (s, 2H), 5.31 (m, 1H), 4.48 (s, br, 2H), 3.11−2.93 (m, 2H), 2.40 (s, 3H), 2.10 (s, 6H), 1.97 (s, 3H), 1.28 (d, 3H, *J* = 6.0 Hz).

Method 2. Into an Et_2O solution of **6** at −78 °C, which was made from **5** (8.1 g, 40.5 mmol) and *n*-BuLi (1.6 M in Hexane, 27.8 mL, 44.5 mmol) in Et_2O (120 mL), was added CH_3CHO (2.5

mL, 44.5 mmol) via a syringe. The reaction mixture was allowed to warm to room temperature over 30 min. The reaction mixture was then cooled down to −78 °C, and ethyl acetate (10 mL) was added. The mixture was allowed to warm to room temperature, and stirring continued for an additional 30 min. The reaction mixture was treated with H_2O (100 mL), and the products were extracted with ethyl acetate (100 mL). The organic solution was washed with brine and water, dried over $NaSO_4$, and the solvent was evaporated under reduced pressure. The crude product was purified with silica gel chromatograph using 1:6, 1:4, and 1:1 ethyl acetate/petroleum ether to afford **7** (3.9 g) and **34** (4.85 g) as colorless liquids.

1-(6-Amino-4-methylpyridin-2-yl)propan-2-yl acetate (35). Compound **35** was synthesized from **34** using the standard deprotection procedure in 55% yield as a light-yellow solid (mp 83−85 °C). ^{1}H NMR (CD_3Cl, 300 MHz) δ 6.37 (s, 1H), 6.19 (s, 1H), 5.25 (m, 1H), 4.48 (s, br, 2H), 2.92−2.68 (m, 2H), 2.20 (s, 3H), 1.99 (s, 3H), 1.25 (d, 3H, J = 6.0 Hz).

1-(6-(*tert*-Butoxycarbonylamino)-4-methylpyridin-2-yl)propan-2-yl acetate (36). A solution of **35** (0.5 g, 2.4 mmol) and di-*tert*-butyl dicarbonate (1.2 g, 5.5 mmol) in *t*-BuOH (15 mL) was stirred in a 65 °C oil bath for 66 h. Solvent was removed under reduced pressure, and the residue was purified by silica gel chromatograph using 1:4 ethyl acetate/hexanes to afford **36** (0.5 g) in 68% yield as colorless liquid. ^{1}H NMR (CD_3Cl, 300 MHz) δ 7.61 (s, 1H), 6.65 (s, 1H), 5.26 (m, 1H), 2.95−2.71 (m, 2H), 2.30 (s, 3H), 1.97 (s, 3H), 1.50 (s, 9H), 1.23 (d, 3H, J = 6.0 Hz).

***tert*-Butyl 6-(2-Hydroxypropyl)-4-methylpyridin-2-ylcarbamate (37).** Into a solution of **36** (0.9 g, 2.9 mmol) in methanol (15 mL) was added a solution of K_2CO_3 (0.8 g, 5.7 mmol) in water (6 mL). The reaction was stirred at room temperature for 2 h and then diluted in water (100 mL) and extracted with ethyl acetate (2 × 50 mL). The organic solution was dried over Na_2SO_4, and the solvent was removed under reduced pressure. The residue was purified by silica gel chromatograph using 1:1 ethyl acetate/hexanes to afford **37** (0.6 g) in 78% yield as white solid (mp 118.0−120.0 °C). ^{1}H NMR (CD_3Cl, 300 MHz) δ 7.66 (s, 1H), 6.63 (s, 1H), 4.15 (m, 1H), 2.81−2.65 (m, 2H), 2.32 (s, 3H), 1.52 (s, 9H), 1.24 (d, 3H, J = 6.0 Hz).

1-(6-(*tert*-Butoxycarbonylamino)-4-methylpyridin-2-yl)propan-2-yl Methanesulfonate (38). Into a solution of **37** (0.25 g, 0.94 mmol) was added triethyl amine (200 μL, 1.44 mmol), followed by methanesulfonyl chloride (80 μL, 1.0 mmol). The reaction mixture was stirred at room temperature for 1 h and then diluted with water (20 mL). The product was extracted with CH_2Cl_2 (2 × 50 mL), and the combined organic layer was dried over Na_2SO_4. After removal of the solvent under reduced pressure, the residue was purified by silica gel chromatograph using 1:2 ethyl acetate/hexanes to afford **38** (0.27 g) in 83% yield as white solid (mp 61−63 °C). ^{1}H NMR (CD_3Cl, 300 MHz) δ 7.66 (s, 1H), 6.69 (s, 1H), 5.16 (m, 1H), 3.03−2.82 (m, 2H), 2.62 (s, 3H), 2.31 (s, 3H), 1.52 (s, 9H), 1.48 (d, 3H, J = 6.3 Hz).

Radiosynthesis of [^{18}F]9. [^{18}F]fluoride (∼180 mCi) was dried by azeotropic distillation using CH_3CN (3 × 1 mL) in the presence of K_2CO_3 (0.75 mg) and K_{222} (5 mg) at 110 °C under a flow of N_2, and then a solution of **38** (2.5 mg) in CH_3CN (400 μL) was added. After the reaction mixture was heated in an oil bath (110 °C) for 10 min [incorporation: 17.3 ± 4.4% (n = 10) according to radio-TLC analysis: silica, 1:1 ethyl acetate/hexanes], it was passed through a silica gel SepPak (Waters) and CH_3CN (2 × 1 mL) was used to rinse the reaction vial and the SepPak. The elution was concentrated to less than 500 μL in the presence of 1 N HCl (100 μL) at 110 °C under a flow of N_2, and then 1 N HCl (500 μL) was added. The reaction mixture was irradiated under microwave for 30 and 25 s with an interval of 30 s between each irradiation and then was diluted in water (3 mL) for HPLC injection. [^{18}F]**9** was purified by reversed-phase HPLC using an Alltech Platinum EPS C18 column (250 mm × 10 mm, 10 μ) eluted with 15% CH_3CN, 85% water with 0.1% trifluoroacetic acid (TFA) at a flow rate of 4 mL/min and UV at 272 nm. The radioactivity (∼8 mCi) corresponding to [^{18}F]**9** was collected at 17 min, and the collection fraction was concentrated under reduced pressure to less than 0.5 mL and then diluted in water (40 mL). [^{18}F]**9** was separated from the dilution by passing the dilution through an Oasis HLB cartridge (Waters) and eluted from the cartridge with ethanol (1−2 mL). If necessary, the ethanol solution was concentrated under a flow of N_2 in order to make a final dose for animal study with <10% ethanol in saline. The total synthesis and purification time was 120 min; decay-corrected radiochemical yield was 6.2 ± 2.1% (n = 10); Radiochemical purity was >99.9%, and specific activity was 2160 ± 1660 mCi/μmol (n = 10) at the end of synthesis, analyzed by an analytical HPLC column (Alltech Platinum EPS C18 250 mm × 4.6 mm, 10 μ, 20% CH_3CH, 80% water, 0.1% TFA, 2 mL/min, 272 nm) and determined by comparison of the integrated UV absorbance with a calibrated mass/UV absorbance curve of **9**. The identity of [^{18}F]**9** was confirmed by the coelution of [^{18}F]**9** with nonradioactive standard **9** on the analytical HPLC system.

NOS Enzyme Assays. All assays were performed using the nitric oxide synthase screening kit (GE Healthcare Biosciences Corp., Piscataway, NJ) following the manufacturer's protocol with minor modifications. Recombinant inducible nitric oxide synthase (iNOS), endothelial nitric oxide synthase (eNOS), and neuronal nitric oxide synthase (nNOS) (Cayman Chemical Company, Ann Arbor, MI) were assayed to establish optimal enzyme concentrations and conditions. In short, all assays were carried out in reaction buffer containing 50 mM Tris pH 7.4, 1.0 mM NADPH, 3.8 μM FMN, 3.8 μM FAD, 3.8 μM tetrahydro-L-biopterin, 2.0 mM dithiothreitol, and 2.0 μM L-arginine, with the exception of the eNOS and nNOS assays, which included 20 μg/mL calmodulin and 1 mM $CaCl_2$ in the reaction buffer to stabilize the enzymes. All chemicals used in the reaction buffer were purchased from EMD Chemicals Inc. (Gibbstown, NJ). Assays were performed at 80 μL per well in 96-well format. All experimental inhibitors were diluted in methanol or water to ensure compatibility with the assay. 100000 cpm or 0.1 μCi [^{3}H]Arginine was added to the enzyme−inhibitor mixture to initiate the reaction. The reaction was allowed to incubate for 30 min at room temperature before it was terminated by the addition of 40 μL of yttrium-silicate SPA arginine binding beads in "stop solution" (50 mg/mL in 50 mM NaOH solution). The arginine binding beads were allowed to settle for 2 h before the plates were counted on a Micro-Beta (PerkinElmer Life and Analytical Sciences, Waltham, MA). Inhibition curves were determined using Kaleidagraph (Synergy Software, Reading, PA). All IC_{50} values were recorded as mean ± SD ($N \geq 3$).

Western Blot Analysis. Lungs from nontreated and LPS-treated C57BL/6N mice (Charles River Laboratories, Wilmington MA) were harvested and homogenized in T-Per tissue protein extraction reagent (Pierce Biotechnology, Rockford, IL) containing Complete protease inhibitor cocktail tablets (Roche Applied Science, Indianapolis, IN) on ice. Homogenates were sonicated 5−10 s 3 times on ice and centrifuged at 12000 rpm at 4 °C for 15 min. Aliquots of protein (200 μg) from each sample were analyzed using standard immunoblotting procedures. The presence of iNOS was probed with monoclonal anti-iNOS primary antibody (Sigma-Aldrich, Inc., St. Louis, MO) at a 1:1000 dilution and horseradish peroxidase-conjugated goat antirabbit IgG (Cell Signaling Technology, Danvers, MA) at 1:3000 dilution. The SuperSignal WestDura Extended Duration Substrate assay kit (Pierce Biotechnology, Rockford, IL) was used to detect the secondary antibody. Loading control was performed with β-actin (Cell Signaling Technology, Danvers, MA).

In Vitro Stability Study. An in vitro stability study was carried out in heparinized whole rat blood (mature male Sprague−Dawley rat). The whole blood (5 mL) was incubated with ∼400 μCi [^{18}F]**9** in 150 μL of saline for 5 min, 30 min, 1 h, and 2 h at 37 °C. An aliquot of blood was treated with 3 volumes of ethanol at each time point, and the lysed sample was centrifuged to separate the supernatant from the pellet. The radioactivity in the supernatant and the pellet was counted separately on a Beckman Gamma 8000 well counter. The radioactive species in the supernatant was analyzed by Silica TLC using ethyl acetate as the developing solvent (R_f = 0.7 for [^{18}Br]**9**) and coelution with nonradioactive **9**.

In Vivo Blood Metabolism Study. The metabolism of [^{18}F]**9** was evaluated in a male Sprague−Dawley rat by iv injection of

[^{18}F]**9** (400 μCi) in 10% ethanol/saline via the tail vein of an anesthetized rat. Blood samples (1.2 mL) were obtained via cardiac puncture under anesthesia at 5 and 30 min postinjection. The plasma was separated from the red blood cells by centrifugation (14000 rpm), and the radioactivity in both samples was measured. After the plasma (400 μL) was treated with 3 equiv of acetonitrile, supernatant and pellet were separated by centrifugation (14000 rpm) and the radioactivity in both samples was measured. The supernatant was filtered through a 0.45 μm nylon filter, and acetonitrile (1 mL) was used to rinse the filter. This supernatant solution was concentrated under a flow of N_2 at room temperature to less than 400 μL. The radioactive species in the supernatant was analyzed by silica gel radio-TLC (developed in ethyl acetate and cospotted with nonradioactive **9**) and reverse phase HPLC (coeluted with **9**). All the samples were kept on ice to prevent degradation.

In Vivo Biodistribution Time-Course Study. All animal experiments were conducted in compliance with the Guidelines for the Care and Use of Research Animals established by Washington University's Animal Studies Committee. The biodistribution study was performed in mature male C57BL/6N mice (age 6−8 weeks) in two experimental groups: one group was intravenously injected with lipopolysaccharide (LPS) (*Escherichia coli* O127:B8, Sigma-Aldrich Co., MO) dissolved in PBS (10 mg/kg, 100 μL per mouse, iv) 6 h prior to the tracer injection to induce iNOS expression; untreated mice were used as control. Reversed-phase HPLC purified [^{18}F]**9** was injected (~50 μCi in 120 μL 10% ethanol/saline, iv) via the tail vein. At the specified time points postinjection (5 min, 30 min, 1 h, and 2 h), the mice were sacrificed, and blood, tissues, and organs were removed, weighed, and counted in a Beckman Gamma 8000 counter with standard diluted aliquots of the injectate. The percent injected dose per gram of tissue (%ID/g) was presented as mean ± standard deviation.

The blocking study was performed following the same procedure described above with the addition of a blocking group (injected with 1400W, 5 mg/kg in saline, iv). [^{18}F]**9** was injected (~5 μCi in 120 μL 10% ethanol/saline, iv) via the tail vein. On the basis of the tracer uptake profile exhibited in the initial biodistribution study and the kinetics of the blocking agent, uptake was evaluated 1 h postinjection. A lower dose of [^{18}F]**9** with higher specificity (4300 mCi/μmol) was used in this study.

MicroPET Study. Two groups of mature male C57BL/6N mice (age 6−8 weeks) were used for the MicroPET study: one set was intratracheally injected with LPS (*Escherichia coli* O127:B8, Sigma-Aldrich Co., MO, 10 mg/kg, 50 μL per mouse, intratracheally) 6 h prior to the tracer injection ($n = 2$); the other set received no treatment and was used as control ($n = 2$). The mice were anesthetized with isoflurane and injected with ~100 μCi/100 μL of [^{18}F]**9** via the tail vein. The imaging sessions were carried out as 1 h dynamic scan using the MicroPET Focus (Siemens Medical Solutions USA, Inc.) scanner. The MicroPET data was then processed using filter back projection algorithm with attenuation and scatter corrections.

Acknowledgment. This research was supported by the National Institutes of Health grants HL13851 and CA 86307.

Supporting Information Available: Combustion analysis data of compounds **9**, **11**, **13**, **15**, **16**, **18**, **20**, **24**, **27**, **30**, **33**, and **38**. This material is available free of charge via the Internet at http://pubs.acs.org.

References

(1) For the latest reviews, see: (a) Mollace, V.; Muscoli, C.; Masini, E.; Cuzzocrea, S.; Salvemini, D. Modulation of prostaglandin biosynthesis by nitric oxide and nitric oxide donors. *Pharmacol. Rev.* **2005**, *57*, 217–252. (b) Alderton, W. K.; Cooper, C. E.; Knowles, R. G. Nitric oxide synthases: structure, function and inhibition. *Biochem. J.* **2001**, *357*, 593–615.

(2) (a) Stuehr, D. J. Mammalian nitric oxide synthases. *Biochim. Biophys. Acta* **1999**, *1411*, 217–230. (b) Marletta, M. A. Nitric oxide synthase structure and mechanism. *J. Biol. Chem.* **1993**, *268*, 12231–12234.

(3) (a) Marletta, M. A.; Hurshman, A. R.; Rusche, K. M. Catalysis by nitric oxide synthase. *Curr. Opin. Chem. Biol.* **1998**, *2*, 656–663. (b) Alderton, W. K.; Cooper, C. E.; Knowles, R. G. Nitric oxide synthases: structure, function and inhibition. *Biochem. J.* **2001**, *357*, 593–615.

(4) Nathan, C. Nitric oxide as a secretory product of mammalian cells. *FASEB J.* **1992**, *6*, 3051–3064.

(5) (a) Titheradge, M. A. Nitric oxide in septic shock. *Biochim. Biophys. Acta* **1999**, *1411*, 437–455. (b) Hobbs, A. J.; Higgs, A.; Moncada, S. Inhibition of nitric oxide synthase as a potential therapeutic target. *Annu. Rev. Pharmacol. Toxicol.* **1999**, *39*, 191–220. (c) Vallance, P.; Leiper, J. Blocking NO synthesis: how, where and why? *Nat. Rev. Drug Discovery* **2002**, *1*, 939–950. (d) Moore, D. J.; West, A. B.; Dawson, V. L.; Dawson, T. M. Molecular pathophysiology of Parkinson's disease. *Annu. Rev. Neurosci.* **2005**, *28*, 57–87. (e) Li, H.; Förstermann, U. Nitric oxide in the pathogenesis of vascular disease. *J. Pathol.* **2000**, *190*, 244–254. (f) Xu, W.; Liu, L. Z.; Loizidou, M.; Ahmed, M.; Charles, I. G. The role of nitric oxide in cancer. *Cell Res.* **2002**, *12*, 311–320.

(6) Lechner, M.; Lirk, P.; Rieder, J. Inducible nitric oxide synthase (iNOS) in tumor biology: the two sides of the same coin. *Semin. Cancer Biol.* **2005**, *15*, 277–289.

(7) (a) Narayanan, K.; Spack, L.; McMillan, K.; Kilbourn, R. G.; Hayward, M. A.; Masters, B. S.; Griffith, O. W. *S*-Alkyl-L-thiocitrullines. Potent stereoselective inhibitors of nitric oxide synthase with strong pressor activity in vivo. *J. Biol. Chem.* **1995**, *270*, 11103–11110. (b) Moore, W. M.; Webber, R. K.; Jerome, G. M.; Tjoeng, F. S.; Misko, T. P.; Currie, M. G. L-*N*6-(1-Iminoethyl)lysine: a selective inhibitor of inducible nitric oxide synthase. *J. Med. Chem.* **1994**, *37*, 3886–3888. (c) Moore, W. M.; Webber, R. K.; Fok, K. F.; Jerome, G. M.; Connor, J. R.; Manning, P. T.; Wyatt, P. S.; Misko, T. P.; Tjoeng, F. S.; Currie, M. G. 2-Iminopiperidine and other 2-iminoazaheterocycles as potent inhibitors of human nitric oxide synthase isoforms. *J. Med. Chem.* **1996**, *39*, 669–672. (d) McCall, T. B.; Feelisch, M.; Palmer, R. M.; Moncada, S. Identification of *N*-iminoethyl-L-ornithine as an irreversible inhibitor of nitric oxide synthase in phagocytic cells. *Br. J. Pharmacol.* **1991**, *102*, 234–238. (e) Furfine, E. S.; Harmon, M. F.; Paith, J. E.; Knowles, R. G.; Salter, M.; Kiff, R. J.; Duffy, C.; Hazelwood, R.; Oplinger, J. A.; Garvey, E. P. Potent and selective inhibition of human nitric oxide synthases. Selective inhibition of neuronal nitric oxide synthase by *S*-methyl-L-thiocitrulline and *S*-ethyl-L-thiocitrulline. *J. Biol. Chem.* **1994**, *269*, 26677–26683. (f) Narayanan, K.; Spack, L.; McMillan, K.; Kilbourn, R. G.; Hayward, M. A.; Masters, B. S.; Griffith, O. W. *S*-Alkyl-L-thiocitrullines. Potent stereoselective inhibitors of nitric oxide synthase with strong pressor activity in vivo. *J. Biol. Chem.* **1995**, *270*, 11103–11110. (g) Southan, G. J.; Szabo, C.; Thiemermann, C. Isothioureas: potent inhibitors of nitric oxide synthases with variable isoform selectivity. *Br. J. Pharmacol.* **1995**, *114*, 510–516.

(8) (a) Young, R. J.; Beams, R. M.; Carter, K.; Clark, H. A.; Coe, D. M.; Chambers, C. L.; Davies, P. I.; Dawson, J.; Drysdale, M. J.; Franzman, K. W.; French, C.; Hodgson, S. T.; Hodson, H. F.; Kleanthous, S.; Rider, P.; Sanders, D.; Sawyer, D. A.; Scott, K. J.; Shearer, B. G.; Stocker, R.; Smith, S.; Tackley, M. C.; Knowles, R. G. Inhibition of inducible nitric oxide synthase by acetamidine derivatives of hetero-substituted lysine and homolysine. *Bioorg. Med. Chem. Lett.* **2000**, *10*, 597–600. (b) Garvey, E. P.; Oplinger, J. A.; Furfine, E. S.; Kiff, R. J.; Laszlo, F.; Whittle, B. J.; Knowles, R. G. 1400W is a slow, tight binding, and highly selective inhibitor of inducible nitric oxide synthase in vitro and in vivo. *J. Biol. Chem.* **1997**, *272*, 4959–4963. (c) Strub, A.; Ulrich, W. R.; Hesslinger, C.; Eltze, M.; Fuchss, T.; Strassner, J.; Strand, S.; Lehner, M. D.; Boer, R. The novel imidazopyridine 2-[2-(4-methoxy-pyridin-2-yl)-ethyl]-3*H*-imidazo[4,5-*b*]pyridine (BYK191023) is a highly selective inhibitor of the inducible nitric oxide synthase. *Mol. Pharmacol.* **2006**, *69*, 328–337. (d) Beaton, H.; Hamley, P.; Nicholls, D. J.; Tinker, A. C.; Wallace, A. V. 3,4-Dihydro-1-isoquinolinamines: a novel class of nitric oxide synthase inhibitors with a range of isoform selectivity and potency. *Bioorg. Med. Chem. Lett.* **2001**, *11*, 1023–1026. (e) Naka, M.; Nanbu, T.; Kobayashi, K.; Kamanaka, Y.; Komeno, M.; Yanase, R.; Fukutomi, T.; Fujimura, S.; Seo, H. G.; Fujiwara, N.; Ohuchida, S.; Suzuki, K.; Kondo, K.; Taniguchi, N. A potent inhibitor of inducible nitric oxide synthase, ONO-1714, a cyclic amidine derivative. *Biochem. Biophys. Res. Commun.* **2000**, *270*, 663–667.

(9) (a) Faraci, W. S.; Nagel, A. A.; Verdries, K. A.; Vincent, L. A.; Xu, H.; Nichols, L. E.; Labasi, J. M.; Salter, E. D.; Pettipher, E. R. 2-Amino-4-methylpyridine as a potent inhibitor of inducible NO synthase activity in vitro and in vivo. *Br. J. Pharmacol.* **1996**, *119*, 1101–1108. (b) Pettipher, E. R.; Hibbs, T. A.; Smith, M. A.; Griffiths, R. J. Analgesic activity of 2-amino-4-methylpyridine, a novel NO synthase inhibitor. *Inflamm. Res.* **1997**, *46*, S135−S136.

(10) Hagmann, W. K.; Caldwell, C. G.; Chen, P.; Durette, P. L.; Esser, C. K.; Lanza, T. J.; Kopka, I. E.; Guthikonda, R.; Shah, S. K.; MacCoss, M.; Chabin, R. M.; Fletcher, D.; Grant, S. K.; Green, B. G.; Humes, J. L.; Kelly, T. M.; Luell, S.; Meurer, R.; Moore, V.; Pacholok, S. G.; Pavia, T.; Williams, H. R.; Wong, K. K. Substituted 2-ami-

nopyridines as inhibitors of nitric oxide synthases. *Bioorg. Med. Chem. Lett.* **2000**, *10*, 1975–1978.

(11) Connolly, S.; Aberg, A.; Arvai, A.; Beaton, H. G.; Cheshire, D. R.; Cook, A. R.; Cooper, S.; Cox, D.; Hamley, P.; Mallinder, P.; Millichip, I.; Nicholls, D. J.; Rosenfeld, R. J.; St-Gallay, S. A.; Tainer, J.; Tinker, A. C.; Wallace, A. V. 2-Aminopyridines as highly selective inducible nitric oxide synthase inhibitors. Differential binding modes dependent on nitrogen substitution. *J. Med. Chem.* **2004**, *47*, 3320–3323.

(12) (a) Zhang, J.; McCarthy, T. J.; Moore, W. M.; Currie, M. G.; Welch, M. J. Synthesis and evaluation of two positron-labeled nitric oxide synthase inhibitors, *S*-[^{11}C]methylisothiourea and *S*-(2-[^{18}F]fluoroethyl)isothiourea, as potential positron emission tomography tracers. *J. Med. Chem.* **1996**, *39*, 5110–5118. (b) Tian, H.; Lee, Z. Radiosynthesis of 8-fluoro-3-(4-[^{18}F]fluorophenyl)-3,4-dihydro-1-isoquinolinamine ([^{18}F]FFDI), a potential PET radiotracer for the inducible nitric oxide synthase. *Curr. Radiopharm.* **2008**, *1*, 49–53. (c) de Vries, E. F.; Vroegh, J.; Dijkstra, G.; Moshage, H.; Elsinga, P. H.; Jansen, P. L.; Vaalburg, W. Synthesis and evaluation of a fluorine-18 labeled antisense oligonucleotide as a potential PET tracer for iNOS mRNA expression. *Nucl. Med. Biol.* **2004**, *31*, 605–612.

(13) Peterson, D. J. Carbonyl olefination reaction using silyl-substituted organometallic compounds. *J. Org. Chem.* **1968**, *33*, 780–784.

(14) Bryk, R.; Wolff, D. J. Pharmacological modulation of nitric oxide synthesis by mechanism-based inactivators and related inhibitors. *Pharmacol. Ther.* **1999**, *84*, 157–178.

(15) Tiso, M.; Strub, A.; Hesslinger, C.; Kenney, C. T.; Boer, R.; Stuehr, D. J. BYK191023 (2-[2-(4-methoxy-pyridin-2-yl)-ethyl]-3*h*-imidazo[4,5-*b*]pyridine) is an NADPH- and time-dependent irreversible inhibitor of inducible nitric-oxide synthase. *Mol. Pharmacol.* **2008**, *73*, 1244–1253.

(16) Speyer, C. L.; Neff, T. A.; Warner, R. L.; Guo, R. F.; Sarma, J. V.; Riedemann, N. C.; Murphy, M. E.; Murphy, H. S.; Ward, P. A. Regulatory effects of iNOS on acute lung inflammatory responses in mice. *Am. J. Pathol.* **2003**, *163*, 2319–2328. (a) Liu, S. F.; Adcock, I. M.; Old, R. W.; Barnes, P. J.; Evans, T. W. Differential regulation of the constitutive and inducible nitric oxide synthase mRNA by lipopolysaccharide treatment in vivo in the rat. *Crit. Care Med.* **1996**, *24*, 1219–1225. (b) Buttery, L. D.; Evans, T. J.; Springall, D. R.; Carpenter, A.; Cohen, J.; Polak, J. M. Immunochemical localization of inducible nitric oxide synthase in endotoxin-treated rats. *Lab Invest.* **1994**, *7*, 755–764. (c) Kan, W.; Zhao, K. S.; Jiang, Y.; Yan, W.; Huang, Q.; Wang, J.; Qin, Q.; Huang, X.; Wang, S. Lung, spleen, and kidney are the major places for inducible nitric oxide synthase expression in endotoxic shock: role of p38 mitogen-activated protein kinase in signal transduction of inducible nitric oxide synthase expression. *Shock* **2004**, *21*, 281–287.

(17) Moncada, S.; Higgs, E. A. Molecular mechanisms and therapeutic strategies related to nitric oxide. *FASEB J.* **1995**, *9*, 1319–1330.

(18) (a) Kovách, A. G.; Szabó, C.; Benyó, Z.; Csáki, C.; Greenberg, J. H.; Reivich, M. Effects of NG-nitro-L-arginine and L-arginine on regional cerebral blood flow in the cat. *J. Physiol.* **1992**, *449*, 183–196. (b) Benyó, Z.; Kiss, G.; Szabó, C.; Csáki, C.; Kovách, A. G. Importance of basal nitric oxide synthesis in regulation of myocardial blood flow. *Cardiovasc. Res.* **1991**, *25*, 700–703. (c) Gardiner, S. M.; Compton, A. M.; Bennett, T.; Palmer, R. M.; Moncada, S. Control of regional blood flow by endothelium-derived nitric oxide. *Hypertension* **1990**, *15*, 486–492.

(19) Alderton, W. K.; Angell, A. D.; Craig, C.; Dawson, J.; Garvey, E.; Moncada, S.; Monkhouse, J.; Rees, D.; Russel, R. J.; Schwartz, S.; Waslidge, N.; Knowles, R. G. GW274150 and GW273629 are potent and highly selective inhibitors of inducible nitric oxide synthase in vitro and in vivo. *Br. J. Pharmacol.* **2005**, *145*, 301–312.

(20) Newman, Melvin, S.; Waltcher, I.; Ginsberg, H. F. The synthesis and reduction of some polyfunctional acetylene compounds. *J. Org. Chem.* **1952**, *17*, 962–970.

JM801556H